

# Air Leakage Detection in Building Façades by Combining Lock-In Thermography with Blower Excitation

Benedikt Kölsch\*<sup>1</sup>, Johannes Pernpeintner<sup>2</sup>, Björn Schiricke<sup>2</sup>, and Eckhard Lüpfer<sup>2</sup>

*1 German Aerospace Center (DLR)  
Institute of Solar Research  
Karl-Heinz-Beckurts-Str. 13  
52428 Jülich, Germany*

*2 German Aerospace Center (DLR)  
Institute of Solar Research  
Linder Höhe  
51147 Cologne, Germany*

\*Corresponding author: [benedikt.koelsch@dlr.de](mailto:benedikt.koelsch@dlr.de)

## ABSTRACT

Air leakage in building envelopes is responsible for a large portion of the building's heating and cooling requirements. Therefore, fast and reliable detection of leaks is crucial for improving energy efficiency.

This paper presents a new approach to determining air leakages in a building's envelope from the outside, combining lock-in thermography and thermal excitation by a blower door system. The blower creates a periodic overpressure within the building, inducing periodic temperature variations of the surfaces near the leaks on the outside surface, the façade. With the temperature variations excited at a known frequency, Fourier transforms of the time-series of the thermal images at the excitation frequency result in amplitude and phase images highlighting the areas affected by leaks. Periodic excitation and detection by an IR camera is known as lock-in thermography and is widely used to characterize semiconductor devices and in non-destructive testing. Excitation is usually achieved by optical, electrical, or mechanical energy input.

For this work, measurements of outside façades have been performed with three excitation cycles of a period of 40 seconds at a 75 Pa pressure difference, leading to a total measurement time of only 2 minutes. Measurements have been performed with air temperature differences of 5 to 7 K at highly variable conditions of irradiance, wind, and cloud cover. The measurements show higher detection quality and less impact from changing ambient conditions than the state-of-the-art differential infrared thermography measurements. With the method highlighting the variations in the amplitude image only at the excitation frequency, variations caused by environmental effects are filtered out. A temperature difference as low as a few Kelvin is therefore sufficient, and large façades can be examined from the outside. This amplitude image is already clearer than an image created with differential thermography. A further reduction of unwanted artefacts in the image is demonstrated using phase-weighting of the amplitude by scalar product.

## KEYWORDS

Lock-In, Thermography, Blower Door, Airtightness, Leak Detection, Building Envelope, Building Energy Efficiency

## 1 INTRODUCTION

Uncontrolled airflow through building envelopes is responsible for 30-50 % of a building's heating energy consumption (Kalamees, 2007; Jokisalo et al., 2009; Jones et al., 2015). Thus, the assessment of airtightness, particularly a fast and reliable localization of leaks, is crucial for reducing heating energy demands.

The fan pressurization method, or blower-door test, is specified in several international standards (Deutsches Institut für Normung e. V., 2018; ASTM, 2019) and measures the integral airtightness of buildings. However, the localization of leaks is cumbersome and requires

experience and persistence. For the detection, additional equipment, e.g., smoke generators or anemometers, is needed.

It is also possible to find leaks with infrared thermography (IRT). Building IRT is a common method of visualizing the temperature distribution of the building envelope's surface. Temperature is derived from measured infrared radiation and physical properties (e.g., emittance) of the surface, surrounding conditions, and the measurement system itself. This makes a visual inspection of defects, such as leaks, thermal bridges, and insulation defects in the building envelope easy.

A measurement method combining both building IRT and fan pressurization method is described in the DIN EN 13187 standard (Deutsches Institut für Normung e. V., 1999). The application of the fan (cf. Figure 1a) allows for a defined, high-pressure difference between the building and ambience, resulting in controlled local airflow through the leaks. The building envelope can be investigated from the inside or the outside depending on the placement of the IR-Camera and application of over- or under-pressure. Also necessary is a difference in air temperature between inside and outside, which leads to a temperature change of surface near the leaks, that can be detected by the IR camera. The comparison to reference images from before the fan was activated – referred to as active IRT – allows for a distinction between heat bridges and air leakages. Usually, a room under investigation is depressurized, and ambient air enters the room through the leaks, affecting the temperature of the adjacent surfaces. These temperature changes are recorded by an IR camera. A differential image, subtracting the thermal images before and after operating the blower, highlights changes in the scene, therefore the leaks. The time between images using differential thermography is not described in the standard. Many authors (Lerma et al., 2018; Mahmoodzadeh et al., 2020) used this active IRT for localization of the air infiltrations in buildings. Kalamees et al. (Kalamees, 2007) investigated leaks at a building's inner surface using differential thermography after the pressure difference was applied for 30 min.

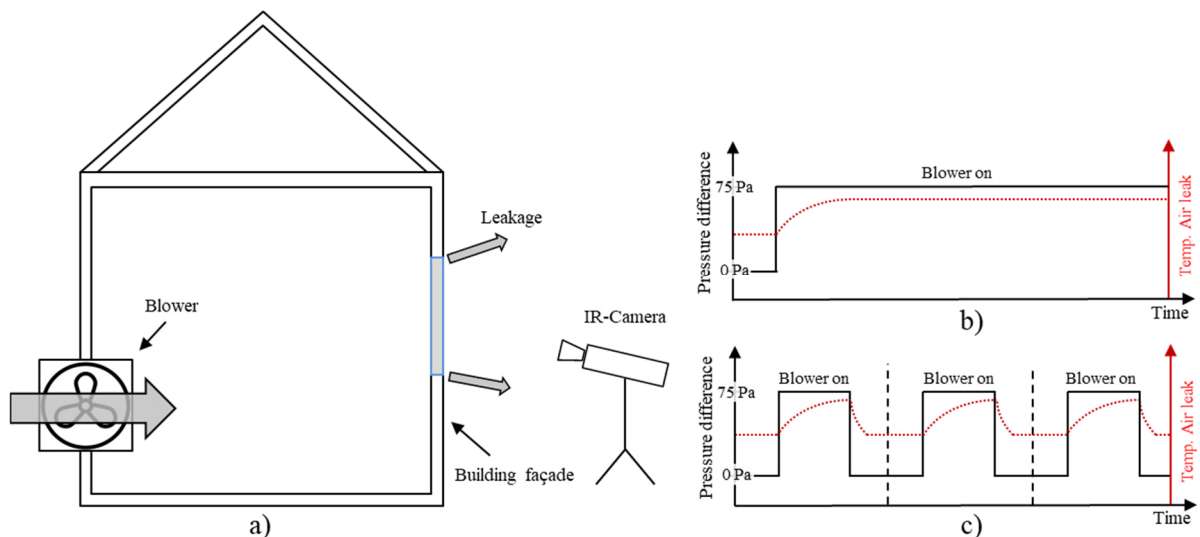


Figure 1: Measurement setup (a), the principle of pressure difference (grey), and anticipated temperature profile of air at leakage (red) using differential thermography (b) and lock-in thermography combined with a blower (c)

However, the infrared image of the building's outside surface is influenced by environmental conditions. Hence, variations of these influences, like wind, irradiation, shadow casting, sky cover, or moving objects in the background between the acquisition of reference and measurement image, are also detected. For this reason, inspections with active IRT are often conducted on the inside facing side of the building's envelope. The temperature difference between inside and outside is recommended to be at least 5 K, better 10 K (Wahlgren and

Sikander, 2010). Scanning an entire façade from the outside remains a desirable goal, as this contains the prospect of a faster and more cost-effective measurement. Fox et al. (Fox et al., 2015) introduced time-lapse thermography, which tracks the temperature changes on building outside walls over a duration of 15-63 h and allows the detection of minimal temperature changes.

Commercial software (BlowerDoor GmbH, 2018) is available that combines air leak location using pressure differential measurements and thermography. In this process, several recorded thermograms are evaluated in an examination period, and only the changes between these thermograms are visualized. However, this software seems also to be tailored to be used for inside surfaces.

This paper explores the combination of active IRT with lock-in amplification. Lock-in amplifiers are algorithms – or machines – for high-precision measurements developed in the 1940s (Stutt, 1949) to reduce measurement noise (Breitenstein et al., 2018). This is achieved by modulation of the excitation of a system – here the blower door fan – with known frequency; compare Figure 1b and Figure 1c. The measurement, where the IR image constitutes multiple measurements, is recorded as time series. By applying the Fourier transformation to the time series of measurements, one can determine the system’s response to the excitation in amplitude and phase. In the classical application as a lock-in amplifier, the user is primarily interested in quantitative measurements. With the improved availability of infrared cameras, the lock-in concept was also applied to materials and component testing, especially of electronic devices, where it developed into the established lock-in thermography (LIT) technique (Breitenstein et al., 2011). In that application, the object’s surface is periodically excited to induce a temperature change of the surface, e.g., with pulsed lamps, laser, ultrasound, or electrical means. While in the latter case, the amplitude response is also of interest, usually, the phase is the primary carrier of information, as the phase corresponds to the penetration depth of the temperature wave, which allows for the detection of bonding defects and delamination in devices.

As the main obstacles to active IRT at the outside building façade are disturbances like wind, sun, etc., and the detection limit of small leaks is primarily given by the signal-to-noise ratio, the lock-in amplification provides an appropriate means to improve the signal-to-noise ratio and to filter out disturbances at other frequencies.

## 2 METHOD

### 2.1 Fourier Transform

The measurement setup is shown in Figure 1a. A blower pressurises a building in regular intervals with a periodic time of excitation  $T_{p,e}$ , equivalent to an angular frequency of  $\omega_e = 2\pi/T_{p,e}$  and a frequency of  $f_e = 1/T_{p,e}$ . The IR camera images the façade. For each pixel of the façade’s image, a time series of temperature values  $T_0$  to  $T_N$  is measured at regularly spaced times  $t_0$  to  $t_N$ . The lock-in algorithm is implemented in this case by calculation of the discrete Fourier transform  $\tilde{T}_k$  for each pixel (compare Figure 2) and frequency given by

$$\tilde{T}_k = \sum_{n=0}^{N-1} T_n \exp\left(-\frac{i 2\pi}{N} kn\right) = Re_k + i Im_k, \quad k = 0, 1, \dots, N - 1 \quad (1)$$

which can be separated into a real part  $Re_k$  and an imaginary part  $Im_k$ .

Amplitude  $A_k$  and phase response  $\varphi_k$  can be calculated by

$$A_k = \sqrt{Re_k^2 + Im_k^2} \quad (2)$$

$$\varphi_k = \tan^{-1}\left(\frac{Im_k}{Re_k}\right) \quad (3)$$

As seen from Eq. 1, the discrete Fourier transform yields a system response at the angular frequencies  $\omega_k = 2\pi k / (t_{N+1} - t_0)$ . Hence, to yield a result exactly at the excitation frequency  $\omega_e$ , the time period  $t_{N+1} - t_0$  must fulfil the relationship

$$t_{N+1} - t_0 = k T_{p,e} \quad (4)$$

where  $k$  represents a whole number as introduced in Eq. 1.

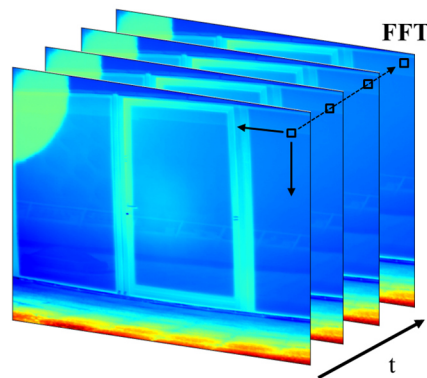


Figure 2: Visualization of FFT calculation for each pixel in their IR time series

Results can be visualized as images of amplitude  $A_k$  and phase  $\varphi_k$ . The unprocessed phase image, however, in lock-in thermography usually the most expressive means to visualize processes, does not appear to be useful here. On the other hand, the amplitude image makes leaks visible at high contrast. However, the amplitude image still shows features resulting from changes in the environment during the measurement if they have some frequency component at the excitation frequency. As these features have – in general – not the same phase as the leaks, a phase-weighted amplitude is defined to investigate further the possibility of suppressing these unwanted features in the image.

## 2.2 Phase-weighted amplitude by Scalar Product

The Fourier transform  $\tilde{T}_k$  can be interpreted as a vector  $\vec{\tilde{T}}_k$  in the complex plane, see Figure 3.

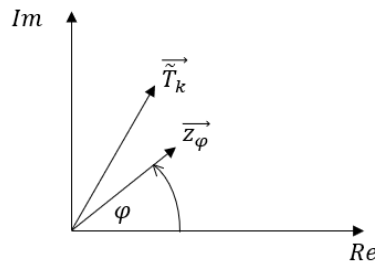


Figure 3: Representation of Fourier transform- and evaluation phase as a vector in the complex plane

The Fourier transform vector  $\vec{T}_k$  shall be evaluated at phase  $\varphi$ . Hence, an additional evaluation vector  $\vec{z}_\varphi$  with length 1 is introduced, which can be written as a complex number  $z_\varphi = \cos \varphi + i \sin \varphi$ . The phase-weighted amplitude  $A_{k,\varphi}$  shall be defined using the scalar product of  $\vec{T}_k$  and  $\vec{z}_\varphi$  by

$$A_{k,\varphi} := \begin{cases} \vec{T}_k \cdot \vec{z}_\varphi = Re_k \cos \varphi + Im_k \sin \varphi & \text{if } \vec{T}_k \cdot \vec{z}_\varphi > 0 \\ 0 & \text{if } \vec{T}_k \cdot \vec{z}_\varphi < 0 \end{cases} \quad (5)$$

The goals of the definition in Eq. 5 are to preserve the amplitude  $A_k$  for parallel vectors  $\vec{z}_\varphi$  and  $\vec{T}_k$  and to yield zero for negative scalar products.

### 3 MEASUREMENT CONFIGURATION

The goal of a measurement campaign performed in October 2021 was the demonstration of lock-in thermography in combination with a blower door system at a building and to compare the results to state-of-the-art differential thermography measurements.

All measurements were carried out at the roof terrace of a large multi-storey office building built in the 1970s, located in the city of Sankt Augustin, Germany. During all measurements, the camera remained stationary outside the building. Figure 4a shows a vis-image of the façade. The imaged part consists primarily of large windows of the height of the total level. The middle window can be opened like a door. Also, in the image is at the bottom of the floor of a terrace and at the top a small part of a protruding roof.

For these tests, additional plastic strips were pinched at two points on the door frame seal, creating artificial and reproducible leaks in the building envelope to be detected (black circles in Figure 4a). Figure 4b shows a representative IR image. The IR images were taken with an InfraTec Image IR 8380 camera with a spectral range between 2 and 5  $\mu\text{m}$  and a resolution of 640x512 pixels. No leaks are visible in the IR image. The circular feature in the upper left corner of the image is an internal reflection within the camera's optics. The glass surface of the windows shows reflections of the terrace opposite to the window. Figure 4c shows the installation of the blower door system at the door of the room adjacent to the window under investigation. The temperature difference between inside and outside was between 5 and 7 K for all measurements. During the measurement, weather was highly variable, with phases of calm and gusty wind and partial cloud cover leading to variable irradiation conditions of direct or diffuse sunlight on the façade. This led to – in conditions of direct sunlight – shadow casting in the upper part of the imaged façade from the protrusion of the roof.

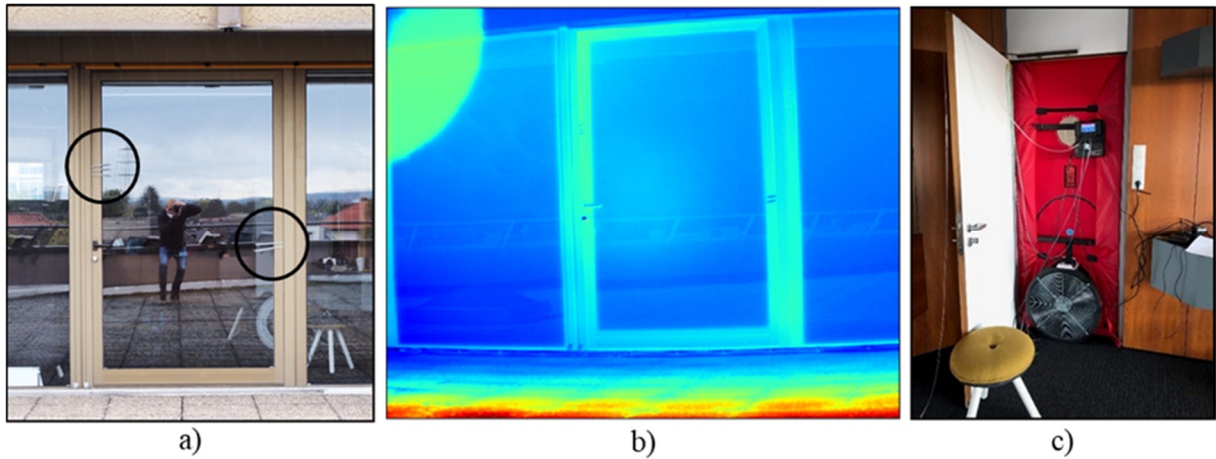


Figure 4: The examined window of the building façade, including inserted plastic stripes – black circles (a), captured IR-image (b), and blower door system in a door frame within the building (c)

For the differential thermography measurements, an initial IR image is taken at the beginning of the measurement period. Then, the blower is switched on, which generates an overpressure of 75 Pa inside the room, leading to an outgoing airflow near the leaks and a change in local air temperature. Another image is taken after a short period of 20 s and a more extended period of 30 min. The basic principle is shown in Figure 1b.

In this measurement campaign, the total duration of the lock-in thermography measurements was 2 min. The IR camera recorded during the entire measurement period. Similar to Figure 1c, 3 periods of  $T_{p,e} = 40$  s were recorded, where the blower is periodically switched on and off for 20 s each. IR images were taken during the measurement period of 2 min with a recording frequency of 2 Hz. Thus, 240 images of the scene were recorded for each measurement.

## 4 RESULTS AND DISCUSSION

### 4.1 Differential infrared thermography

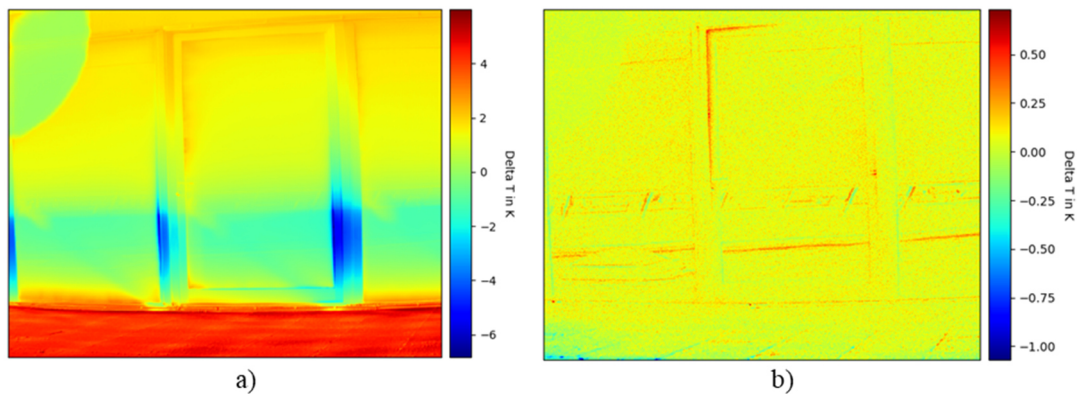


Figure 5: Differential IR images after 30 min (a) and 20 s (b)

Figure 5a shows the differential image of the exterior window façade after 30 min operation of the blower, a time difference often used in building testing. The colour scales for Figure 5 and Figure 6a are selected to show minimum and maximum values.

During this period, the blower door system created a constant pressure difference and, therefore, a significant temperature change at the leaks due to generated airflow. However, these temperature changes are not visible in the IR image. A substantial problem with differential

images taken outside a building, compared to inside recording, is the changing weather conditions (e.g., solar radiation, clouds) between acquisition of the images. These externally induced temperature changes on the building surface have, in this case, a much higher impact over this period than the local temperature changes created by the blower door system.

Another differential image (Figure 5b) is taken with a time difference of 20 s. This shorter measurement period dramatically reduced the influence of changing weather conditions on the measurement. At the positions of the plastic strips, temperature differences of  $\sim 0.5$  K can hardly be seen. Clearly visible, however, is a large leak at the window frame's upper left corner, where the plastic strips open the window. Additionally, the image shows several features in the reflections of the glass, artefacts of changing ambient conditions.

This measurement procedure is a considerable improvement compared to the measurement with 30 min time difference and functions as a benchmark for the following lock-in thermography measurements.

**4.2 Lock-In infrared thermography**

Seven datasets of lock-in measurements were taken. Figure 6 shows the amplitude and phase images (cf. Eq. 2 and 3) of one dataset of the lock-in measurements. With a periodic time of excitation of 40 s, the evaluation takes place at a frequency of 0.025 Hz. The amplitude image (Figure 6a) is similar in structure to the differential image in Figure 5b. It shows the deliberate leaks, where the plastic stripes are inserted, and a larger area in the upper left corner of the window. However, the image is much clearer with a better signal-to-noise ratio. The artefacts are still visible in the image, e.g., reflections on the ground in the front part of the image or reflections of the railings in the window. The phase image is shown in Figure 6b. While the window terrace and railings are clearly visible, the phase image itself does not seem to be useful in highlighting the leaks. However, the phase image does indicate that certain features are connected to specific phases in the Fourier transform.

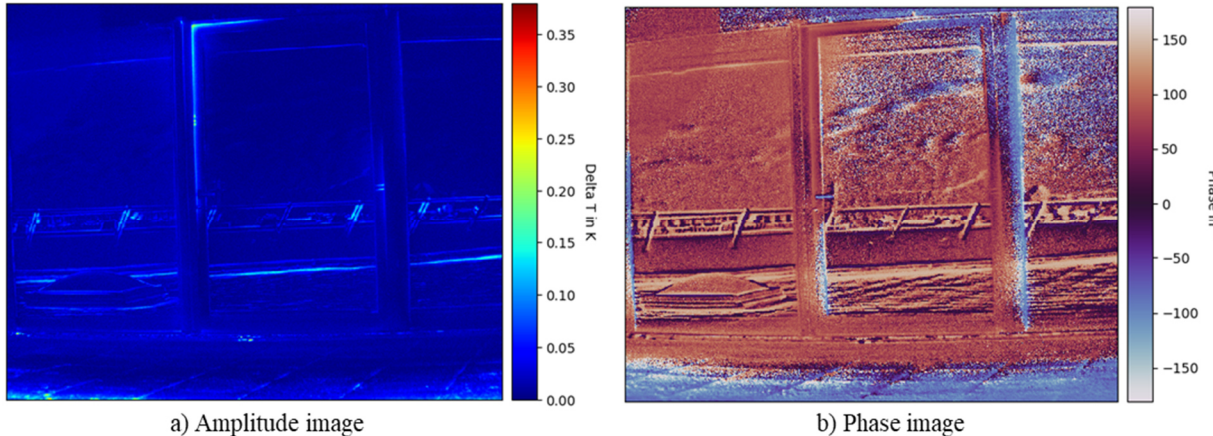


Figure 6: Amplitude pixel values (a) and phase pixel values (b) of FFT at a frequency of 0.025 Hz

Combining amplitude and phase promises to separate different artefacts or temperature changes from different sources in the amplitude image. Thus, a weighting of the amplitude values with phase values is implemented in the following according to the method described in Section 2.2.

Figure 7 shows the results of phase-weighted amplitude for the dataset presented already in Figure 6 at phases  $-180^\circ$ ,  $-120^\circ$ , and  $60^\circ$ . This dataset and these phases are selected specifically as they highlight certain features in the image. For better comparability, the colour scales in Figure 7 are chosen identical as in Figure 6a.

In Figure 7a, the amplitude image is weighted with a phase angle of  $-180^\circ$ , where only the reflections in the window (e.g., the railing) are visible. At a phase angle of  $-120^\circ$  (Figure 7b), the floor area in front of the window is predominantly visible in the image. Finally, at  $60^\circ$  (Figure 7c), solely the leaks in the door frame are evident, and other features are much subdued. Hence, evaluation of the amplitude at a known excitation frequency and characteristic phase angle can be used to separate variations caused by environmental effects and the leaks. This is a significant improvement compared to the amplitude or phase image alone, shown in Figure 6. However, while the phase of the excitation by the blower door is controlled, the phase of variations in the environment is random. Hence, this separation becomes more difficult as the difference between the phase of excitation and environment decreases.

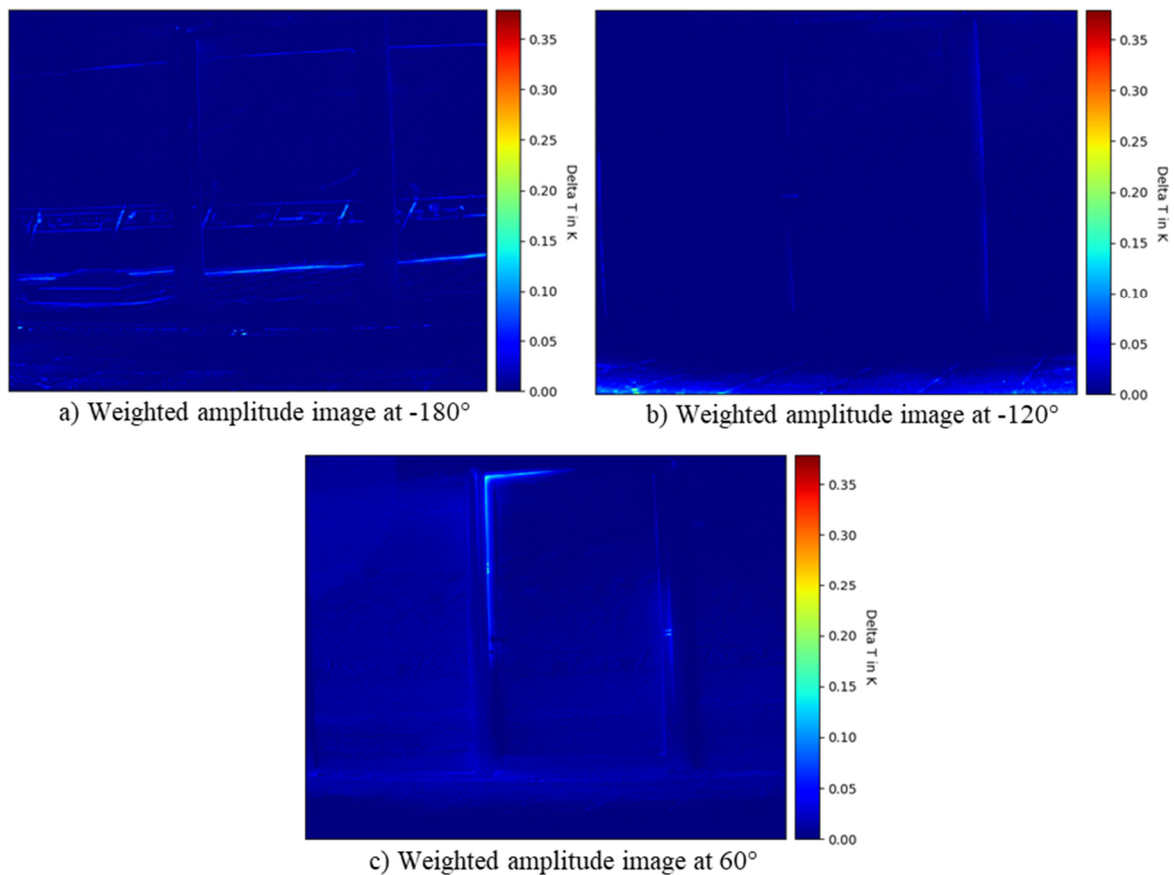


Figure 7: Phase weighted amplitude pixel values for the identical dataset as shown in Figure 6 at selected phase angles of  $-180^\circ$  (a),  $-120^\circ$  (b), and  $60^\circ$  (c)

## 5 CONCLUSIONS AND OUTLOOK

In this paper, the new method of lock-in thermography in combination with a blower door system is applied to building envelopes. This enables a fast identification of air leaks on entire façades. The amplitude image alone shows an improvement in clarity compared to differential thermography. In the illustrated example measurement, it was also possible to separate different excitation sources by evaluating the amplitude image at different phase angles, further improving the results. This new method can be carried out faster than previous state-of-the-art methods and is less sensitive to changing ambient conditions. In addition, this method can be easily standardized, automated, and thus applied to large building façade areas.

However, if the excitation frequency and phase fortuitously match with a temperature fluctuation caused by environmental effects, a separation of the impact is hardly possible yet. More reliable identification and separation of leaks remain for future work.

## 6 REFERENCES

- ASTM (2019). E779-19 Test Method for Determining Air Leakage Rate by Fan Pressurization. West Conshohocken, PA: ASTM International.
- BlowerDoor GmbH (2018). *Bau.Tools BlowerDoor*. Springe-Eldagsen.
- Breitenstein, O., Schmidt, C., Altmann, F. and Karg, D. (2011). Thermal Failure Analysis by IR Lock-in Thermography. In: ASM International (ed.), *Microelectronics Failure Analysis: Desk Reference*, 330–339.
- Breitenstein, O., Warta, W. and Schubert, M.C. (2018). *Lock-in Thermography: Basics and Use for Evaluating Electronic Devices and Materials*. Berlin, Heidelberg: Springer-Verlag.
- Deutsches Institut für Normung e. V. (1999). DIN EN 13187:1998, Thermal Performance of buildings - Qualitative detection of thermal irregularities in building envelopes - Infrared method. Berlin: Beuth Verlag GmbH.
- Deutsches Institut für Normung e. V. (2018). DIN EN ISO 9972:2018-12, Thermal performance of buildings - Determination of air permeability of buildings - Fan pressurization method. Berlin: Beuth Verlag GmbH.
- Fox, M., Coley, D., Goodhew, S. and Wilde, P. de (2015). Time-lapse thermography for building defect detection. *Energy and Buildings*, 92, 95–106.
- Jokisalo, J., Kurnitski, J., Korpi, M., Kalamees, T. and Vinha, J. (2009). Building leakage, infiltration, and energy performance analyses for Finnish detached houses. *Building and Environment*, 44(2), 377–387.
- Jones, B., Das, P., Chalabi, Z., Davies, M., Hamilton, I., Lowe, R., Mavrogianni, A., Robinson, D. and Taylor, J. (2015). Assessing uncertainty in housing stock infiltration rates and associated heat loss: English and UK case studies. *Building and Environment*, 92, 644–656.
- Kalamees, T. (2007). Air tightness and air leakages of new lightweight single-family detached houses in Estonia. *Building and Environment*, 42(6), 2369–2377.
- Lerma, C., Barreira, E. and Almeida, R.M. (2018). A discussion concerning active infrared thermography in the evaluation of buildings air infiltration. *Energy and Buildings*, 168, 56–66.
- Mahmoodzadeh, M., Gretka, V., Wong, S., Froese, T. and Mukhopadhyaya, P. (2020). Evaluating Patterns of Building Envelope Air Leakage with Infrared Thermography. *Energies*, 13(14).
- Stutt, C.A. (1949). *Low-Frequency Spectrum of Lock-In Amplifiers*, Technical Report No. 105, Research Laboratory of Electrics - Massachusetts Institute of Technology. Cambridge, Massachusetts.
- Wahlgren, P. and Sikander, E. (2010). Methods and Materials for an Airtight Building, *Proceedings of the Thermal Performance of the Exterior Envelopes of Whole Buildings XI Conference*.